

LIMNOLOGY AND OCEANOGRAPHY

January 2009

Volume 54

Number 1

Limnol. Oceanogr., 54(1), 2009, 1–12
© 2009, by the American Society of Limnology and Oceanography, Inc.

In situ microscale variation in distribution and consumption of O₂: A case study from a deep ocean margin sediment (Sagami Bay, Japan)

*Ronnie N. Glud*¹

Dustaffnage Marine Laboratory, Scottish Association of Marine Sciences, Oban, Scotland PA37 1QA, United Kingdom;
Marine Biological Laboratory, University of Copenhagen, Strandpromenaden 5, DK-3000 Helsingør, Denmark

Henrik Stahl

Dustaffnage Marine Laboratory, Scottish Association of Marine Sciences, Oban, Scotland P A37 1QA, United Kingdom

Peter Berg

Department of National Environmental Science, University of Virginia, Charlottesville, Virginia 22903

Frank Wenzhöfer

Max Planck Institute for Marine Microbiology, Celcius str 1, 28359 Bremen, Germany

Kazumasa Oguri and Hiroshi Kitazato

Research Program for Paleoenvironment, Institute for Research on Earth Evolution, JAMSTEC, Natsushima 2-15, Yokosuka, Kanagawa, 237-0061, Japan

Abstract

A transecting microprofiler documented a pronounced small-scale variation in the benthic O₂ concentration at 1450-m water depth (Sagami Bay, Japan). Data obtained during a single deployment revealed that within a sediment area of 190 cm² the O₂ penetration depth varied from 2.6 mm to 17.8 mm (average; 6.6 ± 2.5 mm) and the diffusive O₂ uptake, calculated from the vertical concentration gradient within the diffusive boundary layer, ranged from 0.6 mmol m⁻² d⁻¹ to 3.9 mmol m⁻² d⁻¹ (average; 1.8 ± 0.7 mmol m⁻² d⁻¹, $n = 129$). However, correction for microtopography and horizontal diffusion increased the average diffusive O₂ uptake by a factor of 1.26 ± 0.06 . Detailed 2D calculations on the volume-specific O₂ consumption exhibited high variability. The oxic zone was characterized by a mosaic of sediment parcels with markedly different activity levels. Millimeter- to centimeter-sized “hot spots” with O₂ consumption rates up to 10 pmol cm⁻³ s⁻¹ were separated by parcels of low or insignificant O₂ consumption. The variation in aerobic activity must reflect an inhomogeneous distribution of electron donors and suggests that the turnover of material within the oxic zone to a large extent was confined to hot spots. The in situ benthic O₂ uptakes, measured during four cruises, reflected a seasonal signal overlying the observed small-scale variability. The annual benthic mineralization balanced ~50% of the estimated pelagic production. However, the central bay is characterized by a significant downslope sediment transport, and mass balance estimates indicate 90% retention of the total organic material reaching the bottom of the central bay.

¹ Corresponding author (ronnie.glud@sams.ac.uk).

Acknowledgments

We thank the skillful and efficient crews of the Remote Operating Vehicle Hyperdolphin and the R/V *Natushima* for excellent support. Anni Glud is thanked for technical assistance and sensor fabrication. Constructive and valuable suggestions by two anonymous reviewers helped improving the manuscript. Financial support by the Danish Research Council for Nature and Universe, the European Union commission (GOCE-CT2003-505564; RNG, HS), Japan Society for the Promotion of Science (18710021, 17204046; KO, KH), JAMSTEC (KO, KH), and the Max Planck Society (FW) is gratefully acknowledged.

Sediment O_2 uptake represents the most widely used proxy to estimate benthic carbon mineralization and the benthic O_2 availability has major implications for the relative importance of the different mineralization pathways (Thamdrup 2000). Therefore there has been considerable interest in resolving the O_2 distribution of aquatic sediments and to understand factors affecting the benthic O_2 dynamics (Glud 2008). Microelectrodes, micro-optodes, and planar optodes have all proved themselves to be valuable tools for this task (Kuhl and Revsbech 2001), but it has also been realized that to obtain trustworthy data (at least at any significant water depth) measurements have to be performed directly at the seabed (Glud et al. 1994; Epping et al. 2002). In situ microsensors have been applied to large number of benthic environments, but generally technical and logistic constrains limit the number of profiles that can be obtained during a given deployment to 4–8. Multiple microprofile measurements performed on recovered sediment have suggested that the seafloor is characterized by an extensive small-scale variability (Jørgensen et al. 2005) and this has been supported by multiple lander deployments carried out during seasonal studies in shallow-water environments (Glud et al. 2003; Rabouille et al. 2003). Oxygen imaging using planar optodes complements the microprofiling approach by obtaining two-dimensional (2D) high-resolution O_2 images across the sediment water interface. Images typically cover 7×5 cm and, in principle, consist of numerous neighboring micro-profiles, and in situ O_2 images have documented an extensive small-scale variability in the benthic O_2 distribution (Glud et al. 2005). The approach is, however, invasive because an inverted periscope is inserted into the seabed. This affects the local hydrodynamic conditions and the periscope insertion can induce particle smearing along the measuring window. Although planar optodes are excellent tools for laboratory-based investigations and for following temporal in situ dynamics caused by bioturbation, bioirrigation, or pore-water percolation (Precht et al. 2004; Wenzhoefer and Glud 2004; Cook et al. 2007) in situ planar optode investigations of the small-scale O_2 variability along the primary interface can be compromised.

To investigate and evaluate in situ small-scale O_2 variability of benthic communities we have developed a transecting microprofiler allowing multiple sets of micro-profiles to be obtained along a 90-cm-long transect during a single deployment. In the present study we document, evaluate, and discuss the biogeochemical implications of the small-scale O_2 variability resolved in central Sagami Bay. An annual budget for the carbon turnover at this ocean margin sediment is established and discussed by compiling in situ O_2 exchange measurements obtained during four cruises with available literature information on vertical carbon fluxes and sediment accumulation rates for the area.

Methods

Study site—Sagami Bay is a 3000-km² large embayment at Honshu (Japan), which faces the Pacific Ocean (Fig. 1). Towards the northeast the bay is connected to the relatively shallow and eutrophic Tokyo Bay. The bathymetry is

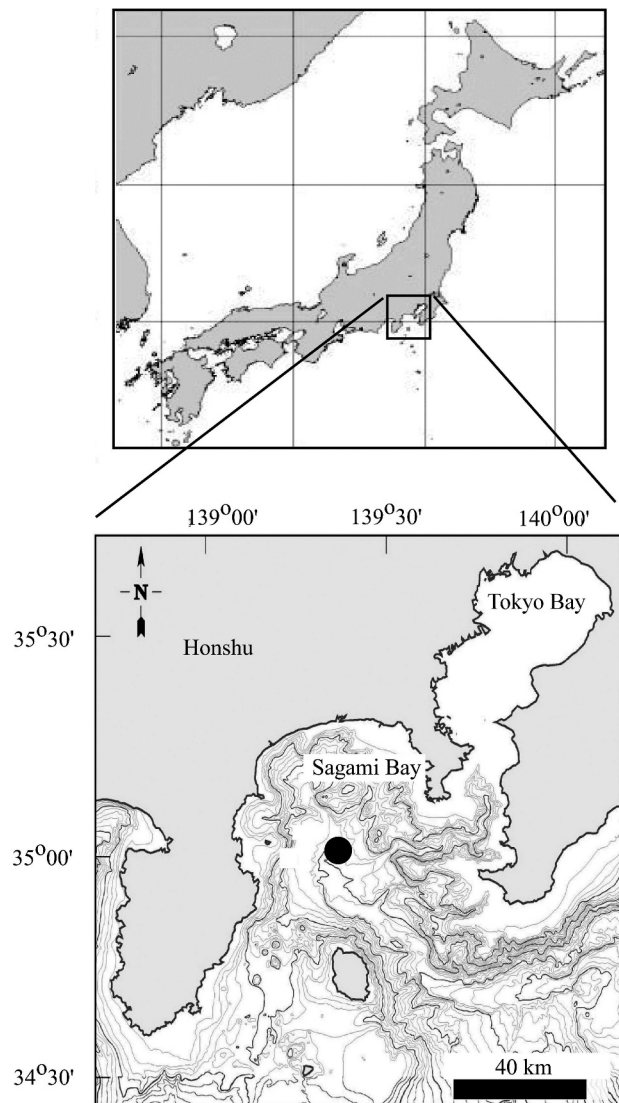


Fig. 1. Sagami Bay with the investigated site (OBBII) indicated by a black dot (modified from Glud et al. 2005). The thick isolines indicate 500-, 1000-, and 1500-m water depth.

dominated by a central canyon extending from the threshold of the Tokyo Bay to the central Sagami Bay with an average water depth around 1500 m (Fig. 1). During 1996–1999 the bay was studied by a large-scale interdisciplinary research program that resolved the temporal variability in the primary production and the pelagic–benthic coupling (Kitazato et al. 2003). The depth-integrated Chlorophyll *a* (Chl *a*) concentration for the upper 50 m typically varied between 20 and 80 mg m⁻² with peak values during a spring and minimum during mid-winter (Kanda et al. 2003). Sediment-trap studies from central Sagami Bay reflect this pattern with a peak in the vertical phytodetritus transport during spring. Hyperpicinal transport of erosion material from the continental slope material does, however, contribute significantly to the net deposition in the central bay (Soh 2003). The intense mineralization of the water column results in O_2 depletion of the water column reaching minimum values around 50 $\mu\text{mol L}^{-1}$ (~15% air-saturation) at 1200–1400-m water depth.

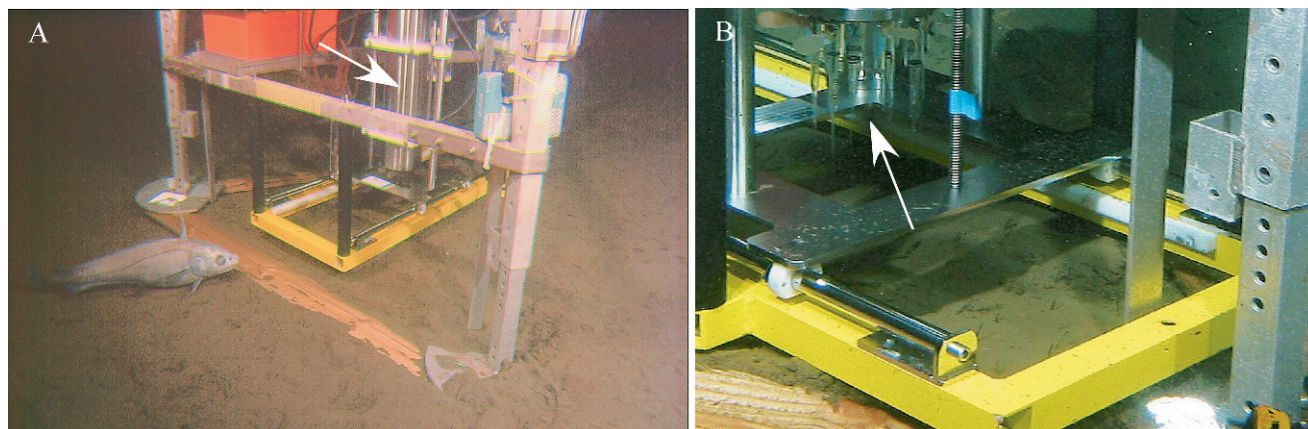


Fig. 2. The transecting profiler was placed at the seabed of central Sagami Bay by the ROV. This procedure ensured absolutely no disturbance of the sediment surface. The electronic cylinder was moved in horizontal increments of 7 mm in between each set of microprofile measurements. Panel A shows the yellow horizontal base hosting the vertical-moving titanium-cylinder (arrow). The wooden frame at the tripod ensured that the instrument did not gradually sink into the sediment during the measurements. Panel B represents a close-up of the sensor array (arrow) immediately above the investigated sediment.

The present study was conducted at 1450-m water depth in central Sagami Bay (35°00.86'N 139°21.59'E—in previous literature referred to as OBBII) from the research vessel R/V *Natsushima*. The vessel acts as mother-ship for the Remotely Operated Vehicle (ROV) Hyperdolphin (www.jamstec.go.jp/jamstec-e/rov/hyper.html), which was used for positioning our transecting profiler, deploying our benthic chamber, and for recovering sediment cores for onboard investigations. Microtransect data were obtained during the period 08–16 December 2006, while additional support data from the same location were measured on three other cruises, which took place 24 September–10 October 2003, 22–27 March 2006, and 17–23 January 2008.

Transecting microprofiler—The central vertical micro-profiling instrument was a slightly updated and modified version of a previously described profiling instrument (Gundersen and Jørgensen 1990; Glud et al. 1994) and was during the present study equipped with four O₂ microelectrodes and one resistivity sensor (*see below*). This instrument was placed on a sledge, which could move a total horizontal distance of 90 cm in increments of 0.7 cm (Fig. 2A,B) obtaining one set of microprofiles at each position. The outer region of the sensor shafts were thinned to ensure that the shaft diameter inserted into the sediment at maximum depth was <1 mm. This eliminated any risks of mechanical interference from neighboring holes during profile measurements. Likewise this horizontal distance eliminated any potential oxygenation from holes created during previous microprofiling to transplant to the measuring site of the next profile.

The whole profiling system was mounted in a benthic lander tripod, which was released from the ship and sank towards the seafloor at a speed of 25 m min⁻¹ (lander weight in water 27 kg). Before the measuring routine was initiated the ROV grabbed the lander from the top and moved the tripod to a site that remained undisturbed from any potential bow-wave (Glud et al. 2005). The lander frame was carefully and slowly lowered by the ROV and

online video recordings confirmed that this was done without any sediment suspension (in one case marginal disturbance was observed and in that case we chose to reposition the instrument). The tripod was equipped with a wooden triangle to avoid sinking into the sediment during the measuring routine. Once the lander was positioned the ROV activated the measuring routine of the transecting profiler by pushing a mechanical switch and after a small delay the electronic cylinder carrying the microelectrodes moved continuously towards the sediment surface. As the resistivity sensor recorded an abrupt 10% drop in the signal indicating the relative position of the sediment surface, the vertical movement stopped and the electronic cylinder receded 3.0 cm. Subsequently, the sledge moved 7 mm horizontally and the electronic cylinder holding the microsensor array was lowered in increments of 0.1 mm for a total distance of 70 mm, before moving back to the initial vertical start position. At each depth the signal of all sensors was recorded and stored by the computer in the pressure housing. The sledge then moved horizontally for another 7 mm and the measuring routine was repeated. The routine was repeated 33 times and the entire measuring procedure required a total deployment time of 28 h (this should potentially provide 132 microprofiles during our deployment but, due to breakage of one sensor towards the end, the actual value was only 129). At the end of the measuring procedure the ROV grabbed and lifted the lander tripod to the sea surface where both instruments were recovered from the mother ship.

Sensor measurements and calculations—The resistivity probe was a custom-made, two-wire sensor with a tip diameter of 0.8 mm. The distance between the two emerging electrode wires was 0.4 mm and tests in homogenized, fine-grained sediment indicated that a signal shift at the surface was resolved at a vertical resolution of 0.4 mm (i.e., the constant signal in the water changed over a distance of 0.4 mm to a lower constant signal of the interstice). The vertical profile of the formation resistivity

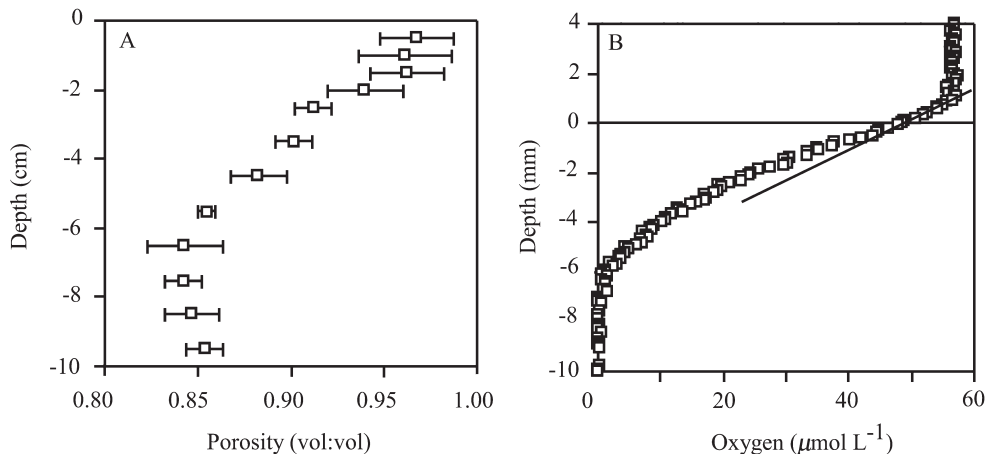


Fig. 3. (A) The average porosity profile ($n = 4$) as measured in sediment recovered by plastic core liners (i.d. 8.2 cm) from central Sagami Bay (OBBII). (B) One typical in situ O₂ microprofile measured at the same site reflecting a break in the slope of the concentration gradient at the sediment surface ($y = 0$), the linear concentration slope within the 940- μm -thick DBL is indicated.

factor, F , was calculated by dividing the sensor signal at each sediment depth, R_s with the constant signal resolved in the bottom water, R_w , (i.e., $F = R_s/R_w$), (Ullman and Aller 1982). Subsequently the effective sediment diffusive transport coefficient, D_e , was calculated as $D_e = D_0/(\phi F)$ where, D_0 , is the temperature-, pressure-, and salinity-corrected molecular diffusivity for O₂ in water and, ϕ , the sediment porosity (Ullman and Aller 1982). The latter was determined at a depth resolution of 0.5 cm from sediment slices as the weight loss after 24 h at 100°C multiplied with the specific density. The average porosity of the upper flocculent 1.5 cm exhibited a relatively constant value of 0.96, but below this horizon the values gradually declined down to ~8-cm depth where they stabilized around 0.84–0.85 (Fig. 3A). The organic carbon content was estimated from the weight loss after ignition at 450°C for 24 h and exhibited maximum values of $8.8 \pm 0.4\%$ - dry weight at the sediment surface, which gradually declined to a constant value of $7.7 \pm 0.1\%$ dry weight ($n = 4$) at 8–10-cm sediment depth (data not shown).

The oxygen microelectrodes were of the Clark-type with an internal reference and a guard cathode, tip diameters of ~10 μm , t_{90} response times <2 s and stirring sensitivities <2% (Revsbech 1989). The linear response of each microelectrode was calibrated using the signals in the bottom water of known O₂ concentration and in sediment layers presumed anoxic as indicated by low constant sensor signals. From the microelectrode profiles the vertical diffusive O₂ uptake (DOU) was calculated from Fick's first law of diffusion $\text{DOU} = D_0 (dC/dx)$, where D_0 , is the molecular diffusion coefficient of O₂ at the in situ temperature, salinity, and hydrostatic pressure, and C is the O₂ concentration at depth x , within the diffusive boundary layer (DBL; Rasmussen and Jørgensen 1992). The relative position of the sediment surface was estimated from each individual profile by a shift in the linear concentration gradient of the DBL (Fig. 3B). The O₂ penetration depth was quantified as the distance between the estimated sediment surface and the depth at which the sensor signal reached a constant low value

(anoxic signal). The vertical alignment of the sensors was resolved at a resolution 0.1 mm by lowering the sensor array in increments towards a stagnant water film and observing when the tips broke the water surface. This procedure ensured that the tips of all O₂ microsensors were confined within a narrow horizontal interval of 3 mm, 2–3 cm behind the resistivity sensor.

Benthic chamber measurements—A small frame of carbon-fiber tubes hosted a circular, benthic Plexiglas chamber (inner diameter [i.d.] 19 cm, height 33 cm). The lid sealing the chamber carried two calibrated custom-made O₂ electrodes, a rotating stirrer, and a one-way valve allowing water to escape as the chamber was pushed into the sediment by the ROV. The water height within the transparent chamber was determined from the ROV camera focusing on measuring sticks glued to the chamber wall. A pressure-stable electronic cylinder recorded the sensor signals and a custom-made, pressure-compensated battery packet ensured that the instrument could operate for up to 35 h. At the end of the incubations the ROV grabbed the chamber frame and brought it back to the research vessel. The Total O₂ Uptake rate (TOU) was calculated from the initial, linear O₂ decline over time accounting for the enclosed water volume and the sediment area (samples recovered for nutrient exchange are reported elsewhere).

Laboratory-based measurements—For laboratory-based measurements and onboard core incubations, sediment was collected by the ROV in core liners with an inner diameter of 8.2 cm, while bottom water was collected in 2-liter Niskin bottles mounted on the ROV. Onboard the mother ship, sediment cores were submerged in the bottom water kept at in situ temperature and in situ O₂ concentration. The in situ O₂ concentration was maintained by continuous flushing with an atmospheric air–dinitrogen mixture regulated via a digital gas mixer (Brooks Instruments, The Netherlands, 5850S). Rotating small magnets, receiving momentum from a large central magnet, were attached

to the core-liner ensured a well-mixed overlying water phase kept at in situ O₂ concentration (Rasmussen and Jørgensen 1992). After 12-h pre-incubation at these conditions O₂ microprofiles were measured as described by Rasmussen and Jørgensen (1992). Previous investigations have documented that pre-incubation facilitates reestablishment of the in situ O₂ distribution in sediment cores that have experienced transient heating or disturbance during core recovery (Glud et al. 1999). Subsequently the cores liners were sealed and water samples for O₂ were recovered at a regular interval over a 4–6-h-long incubation period. The O₂ concentration of the respective samples was determined by Winkler titration (or measured by calibrated O₂ microsensors) and the TOU was calculated as above.

Oxygen consumption rates derived from concentration measures in the sediment—The 2D steady-state mass balance equation for oxygen in the sediment that include transport by molecular diffusion and bioturbation yields

$$\frac{\partial}{\partial x} \left(\phi (D_s + D_B) \frac{\partial C}{\partial x} \right) + \frac{\partial}{\partial y} \left(\phi (D_s + D_B) \frac{\partial C}{\partial y} \right) + R = 0 \quad (1)$$

where C is the pore-water oxygen concentration, x is the depth coordinate, y is the horizontal coordinate, ϕ is the porosity, D_s is the molecular diffusivity corrected for tortuosity, D_B is the bio-diffusivity, and R is the net rate of production (or consumption if R is negative) per unit volume of sediment. For further details on the equation, see Boudreau (1997). Here, we solved the equation for R using a control-volume approach (Berg et al. 2007) and with input derived from measured values of C and $\phi(D_s + D_B)$.

Equation 1 expresses that R depends on the second derivatives of C . This makes estimation of R highly sensitive to noise in our measured C -values which consist of series of vertical O₂ microprofiles, 7 mm apart, and with a depth resolution of 0.1 mm (see details above). To minimize this problem, the profiles were lumped vertically to a coarser depth resolution of 1.5 mm. The horizontal resolution of 7 mm was maintained. Thus, our solutions of Eq. 1 resulted in 2D vertical distributions of oxygen uptake rates with a resolution of 1.5×7 mm.

Values for the term $\phi(D_s + D_B)$ in Eq. 1, which is defined as $D_0/(\phi F)$ (see above), were calculated from one representative measured depth profile of F and used in all estimations of R . For each of the measured O₂ microprofiles, this F -profile was aligned vertically to obtain a correct position of the sediment surface. After this alignment, the F -profile that also was measured with a depth resolution of 0.1 mm was lumped to the coarser depth resolution of 1.5 mm.

Results

Most vertical profiles of the formation-resistivity-factor, F , exhibited a distinct and steep increase just below the sediment surface, gradually reaching a plateau around 1.28 at a sediment depth of 2.5–3.5 cm (Fig. 4A,B). A few profiles reflected penetration of funnels or burrows leading

to a more irregular depth profile and relatively low F -values down to the deepest measuring point (Fig. 4C). In areas not affected by funnels, the F -isolines of the upper sediment layers generally followed the estimated topographic relief of the sediment surface. However, deeper sediment layers occasionally hosted areas of elevated values indicating patches of more compacted sediment 3–4 cm below the sediment surface (Fig. 4D). The calculated total sediment diffusivity, D_e , mirrored the measured F -values, with relatively consistent vertical profiles for the upper cm, and more variable conditions in the deeper sediment layers. Direct observations by the ROV camera and inspections of the recovered sediment showed that the sediment surface was fluffy as also indicated by the high porosity (Fig. 3A). The surface sediment had a D_e value of $\sim 1.2 \times 10^{-5}$ cm² s⁻¹, which roughly declined by 6–8% at a sediment depth of 1 cm (Fig. 4E).

In parallel to the F -profile measurements of Fig. 4 a total of 129 O₂ microprofiles were measured along four mini-transects being ~ 20 cm long. The parallel transects were separated by a few cm and all profiles were thus measured within a sediment area of ~ 190 cm². A total of 18 microprofiles or 14% were visually affected by irrigation activity, but even profiles not showing any direct effect of irrigation reflected extensive small-scale variability (Fig. 5). The O₂ penetration depth along the primary interface varied by a factor >6 from 2.6 mm to 17.8 mm with an average value of 6.6 ± 2.6 mm. The modus of the distribution was, however, somewhat smaller (i.e., in the range of 5–6 mm) due to a few profiles with very large penetration (insert in Fig. 5). The DOU as calculated from the vertical concentration gradient resolved within the DBL ranged from 0.6 mmol m⁻² d⁻¹ to 3.9 mmol m⁻² d⁻¹ with an average value of 1.8 ± 0.7 mmol m⁻² d⁻¹. Plotting the resolved O₂ distribution as isopleths elucidates the extensive small-scale variability and documents the fact that the sediment surface and the oxic zone at the relevant spatial scale exhibit a varied topographic relief (Fig. 6). The microtopographic consequences for benthic O₂ exchange has been discussed in detail by Jørgensen and Des Marais (1990) and Røy et al. (2005); the topographic relief enlarges the sediment area across which diffusive exchange takes place and causes horizontal concentration gradients with the DBL and the sediment, factors that not are accounted for by the generally applied simple one-dimensional DOU calculation. By estimating the average angle of the sediment relief and the overlying DBL in relation to the horizontal plane a geometric correction for the simplified one-dimensional vertical approach can be made (Jørgensen and Des Marais 1990; Røy et al. 2005). Using the four transects of Fig. 4 we calculated the average correction factor accounting for both effects to be 1.26 ± 0.06 . The average DOU accounting for three-dimensional topographic features of the seabed thus increased to 2.3 ± 0.9 mmol m⁻² d⁻¹. This value is higher, but not significantly different from the TOU measured in parallel with our benthic chamber (Table 1).

The highly variable O₂ concentration of the surface sediment (having relative invariable transport coefficients) suggests an uneven distribution and activity of O₂-

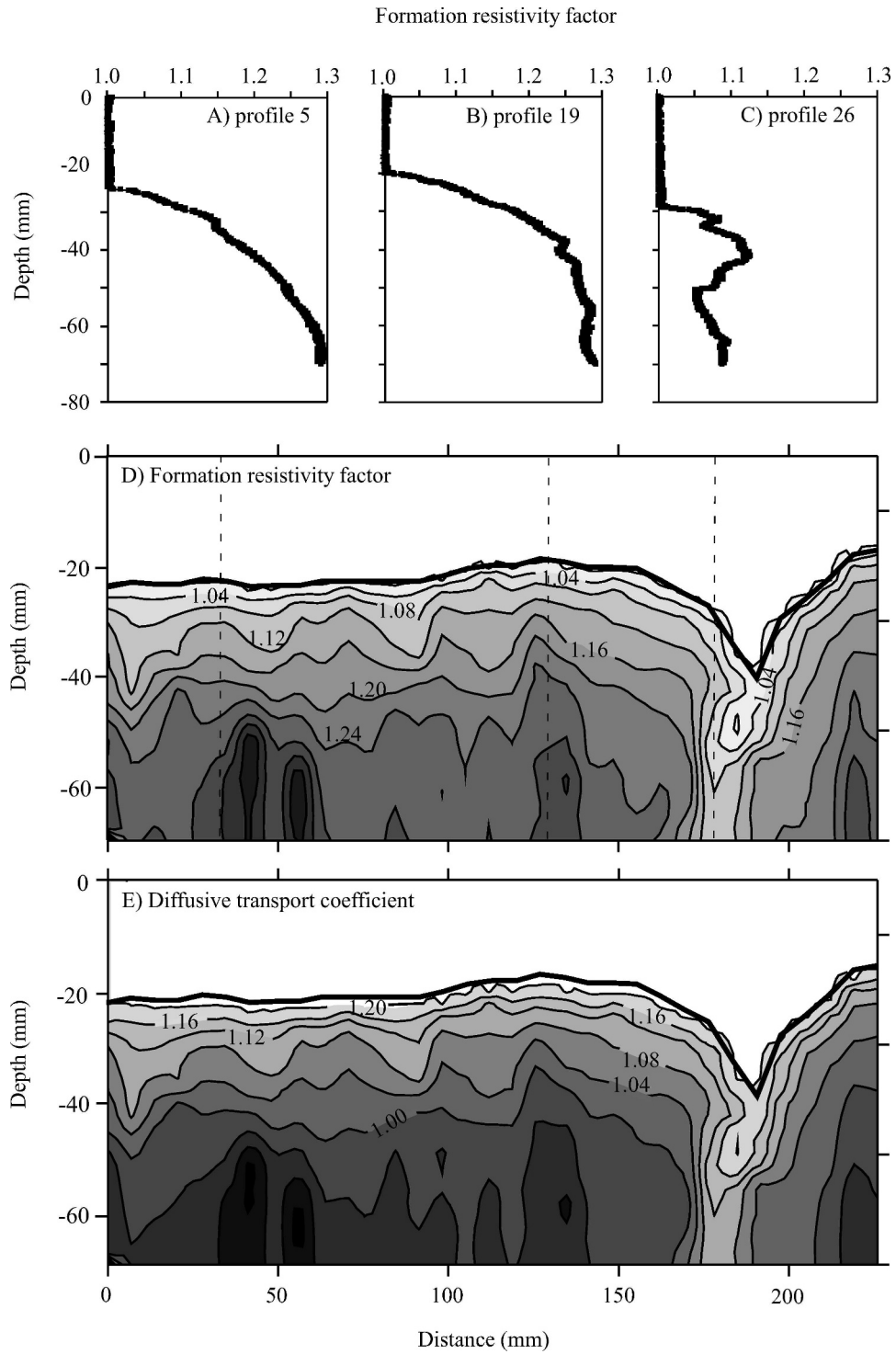


Fig. 4. (A–C) Three selected microprofiles of the formation resistivity factor (F -profiles), profile 5 and 19 are typical whereas profile 26 apparently penetrated an infauna burrow. (D) The 33 F -profiles plotted as an isopleth (isolines represent a step increase of 0.04). The vertical dotted lines indicate the positions of the vertical F -profiles presented in the upper panels. (E) reflects the calculated tortuosity-corrected diffusive transport coefficient of the sediment, D_e , (isolines represent a step increase of $0.04 \times 10^{-5} \text{ cm}^2 \text{ s}^{-1}$).

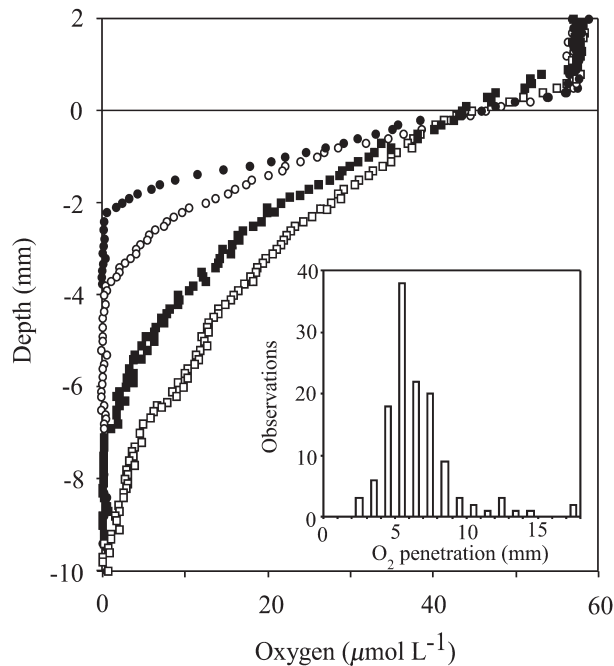


Fig. 5. Selected in situ O₂ microprofiles, which all were measured within the investigated sediment area of ~190 cm². The 0-value at the ordinate indicates the relative position of the estimated sediment surface. The DBL thickness of the profiles ranges between 460 and 960 μm. The insert shows the number of profiles with O₂ penetration depths in respective intervals of 1 mm (i.e., 0–1, 1–2, 2–3... mm); $n = 129$.

consuming processes, R . Due to efficient diffusive transport at small scales even slight variations in the concentration gradients can reflect extensive variations in the O₂ turnover rate. The volume-specific activity of the O₂ consumption was calculated from the O₂ isopleths of Fig. 6 as described above. The results clearly reveal a very heterogeneous O₂ consumption within the surface sediment, characterized by hot spots or zones of intensified activities that are separated by patches of low or insignificant activity (Fig. 7). Occasional penetration of irrigated burrows reflects relatively high O₂ consumption rates just around the burrow (notice how the respective isolines almost merge in panel 7C). Hot spots were occasionally associated to distinct topographic features, as would be expected if they represented recent deposits, but this was not always the case. Sometimes topographic features did not reflect intensified activity and hot spots and zones were also encountered deep inside the oxic zone.

Integrating the calculated O₂ consumption rates for all four transects corresponds to a diffusive O₂ uptake rate across the primary sediment water interface of 2.0 ± 0.4 mmol m⁻² d⁻¹ which is intermediate to the two DBL-derived approaches described above. The horizontal flux within the oxic zone of the sediment ([O₂] > 1 μmol L⁻¹) amounted to $19 \pm 3\%$ (SD) of the vertical flux. The 25% of the oxic volume that hosted the highest activity accounted for $54 \pm 6\%$ of the integrated O₂ consumption rate, while the 25% of the oxic volume having the lowest activity only was responsible for $4 \pm 2\%$ of the integrated O₂

consumption (Fig. 8). This to some extent reflected that deeper oxic layers only hosted a relatively low O₂ consumption rate. On average compartments in the depth range of 1.5–3.0 mm and 3.0–4.5 mm were responsible for 28% and 22% of the total O₂ consumption rate while the very surface (0.0–1.5 mm) accounted for 19% of the O₂ turnover.

Discussion

Microscale benthic O₂ dynamics—Previous investigations have suggested that in homogenous sediments the DOU and the O₂ penetration depth, L , are related as $L = 2\phi D_s(C_w/DOU)$, where C_w is the bottom water concentration of O₂ (Cai and Sayles 1995). A good agreement between this relation and data calculated from selected in situ O₂ microprofiles has previously been used as an indication of steady-state O₂ distribution, uniform distribution of organic material and negligible irrigation in shelf and continental margin sediments (Cai and Sayles 1995). The present data obtained during winter (open symbols) or during late summer 2003 (closed symbols) suggest otherwise (Fig. 9). Whereas the relation reflects the general trend of our data, the scatter strongly suggest an inherent heterogeneity potentially combined with a dynamic O₂ distribution. Data collected during late summer tend to be shifted towards the lower left corner indicating a seasonal shift in the relation (or in the interstitial molecular transport; Fig. 9). The inherent microscale variability of O₂ amplifies into an extensive variation in the O₂ consumption rate within the oxic zone as evident from the calculated volume-specific O₂ consumption rates (Fig. 7) which reflect a mosaic-like distribution of sediment parcels hosting very different activity levels. This observation supports and aligns with previous work at this location performed during the autumn 2003, where it was shown that the O₂ penetration depths, as derived from microelectrode and planar optode data, auto-correlated when measured at spatial distances below 2 cm (Glud et al. 2005). This indicated that the aerobic activity varied in patches with a characteristic size below a few centimeters. Parallel investigations at the same location showed a covariance in the distribution of bacteria and virus, but also exhibited an extreme small-scale variation in the virus and bacteria abundance; in fact, the range in surface abundance of benthic viruses along a 350-m transect at the same location almost covered the global range of published virus abundances for benthic environments (Middelboe et al. 2006). Together these observations clearly suggest that the sediment of central Sagami Bay, rather than being regarded as a laminated structure of microbial communities, has to be envisioned as a mosaic of microbial consortia with very different activity levels. The observation adds to the current discussion on the apparently very high fraction of bacteria that are motile in sediments anticipated to have a relatively uniform distribution of electron donors (Fenchel 2008). The present data indicate that, within the investigated sediment, microbes indeed would benefit from motility and accumulate in optimal local settings. It can be speculated that the extensive spatial variation in O₂ distribution and

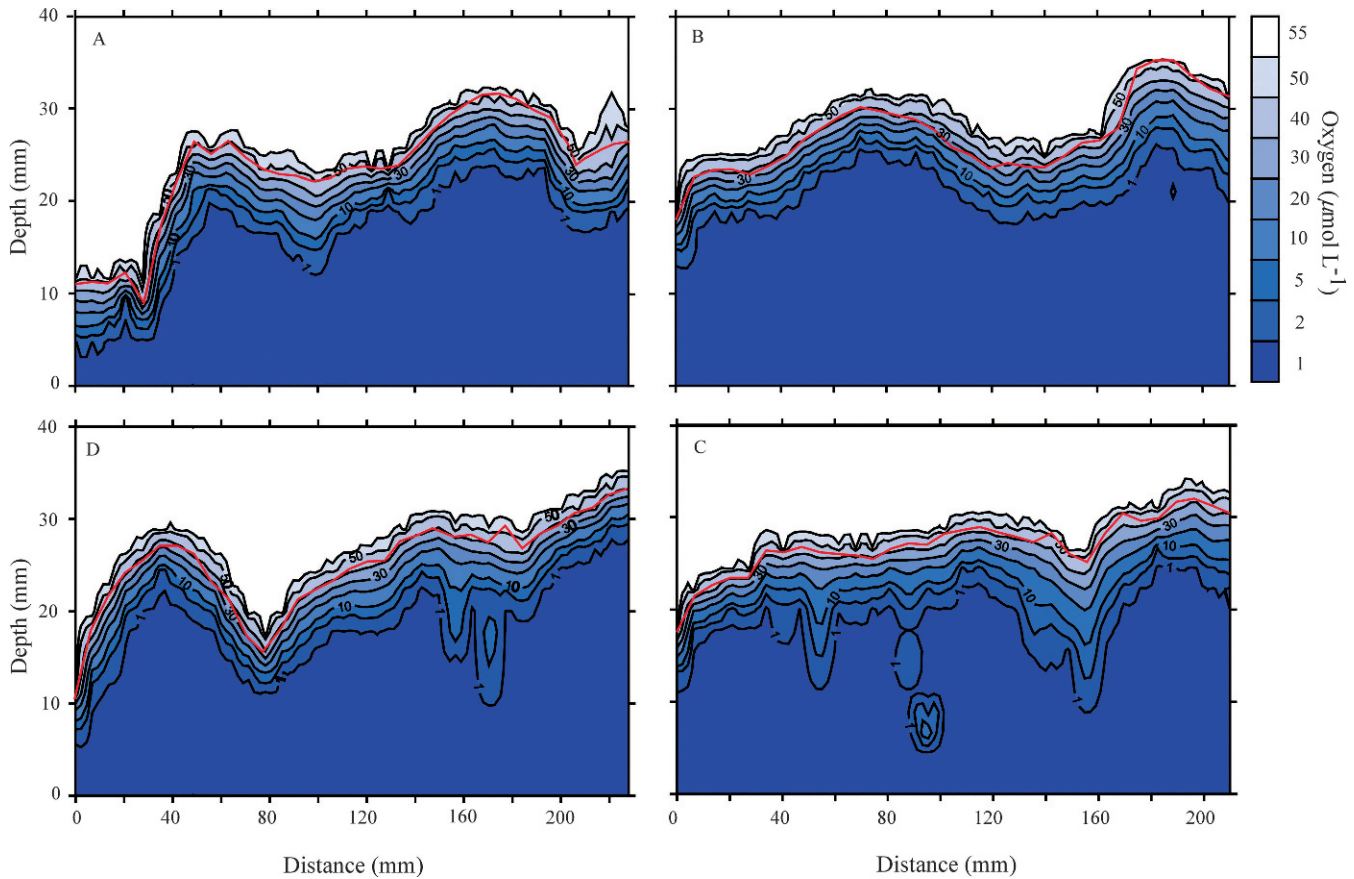


Fig. 6. (A–D) The benthic O_2 distribution along four different parallel transects measured by the transecting microprofiler. The red line indicates the estimated position of the sediment surface.

O_2 consumption also is reflected in the distribution of meiofauna-like ciliates, foraminifera, and nematodes orienting itself in relation to the availability of food and electron acceptors (Fenchel 1996).

It is not possible to outline the processes responsible for the O_2 consumption in the respective patches or zones, but given a relatively high iron respiration and nitrification activity in these sediments (work in progress), it is likely that the O_2 mainly is used by aerobic heterotrophy, iron- and ammonia-oxidation (in situ microsensors measurements showed no free H_2S in the upper 7 cm of the sediment—data not shown). The reason for the patchiness

in O_2 consumption can in part be related to the dense polychaete infauna ($\sim 1000 \text{ m}^2 \pm 200 \text{ m}^2$) as estimated from six recovered sediment cores in January 2008. It is well-established that benthic infauna through their burrowing activity mediate an upward transport of chemically reduced sediment parcels which would lead to localized intensified O_2 consumption within the surface sediment (Aller et al. 1998). Further, infauna activity may induce localized carbon enrichments in the form of fragmented burrow linings or fecal pellets (Zhu et al. 2006). However, another cause for the patchiness in the microbial aerobic activity could be an uneven distribution of sedimenting

Table 1. The total O_2 uptake (TOU) as measured in situ by benthic chambers or in recovered sediment cores, presented together with the diffusive O_2 uptake (DOU) and O_2 penetration depth (L) as derived from O_2 microprofiles measured in parallel either in situ or in the laboratory. The standard deviations are included and “n” indicates the number of replicate measurements (n-values for DOU and O_2 penetration depths are identical).

	In situ			Laboratory		
	TOU ($\text{mmol m}^{-2} \text{d}^{-1}$)	DOU* ($\text{mmol m}^{-2} \text{d}^{-1}$)	L (mm)	TOU ($\text{mmol m}^{-2} \text{d}^{-1}$)	DOU* ($\text{mmol m}^{-2} \text{d}^{-1}$)	L (mm)
03 Sep	-	3.3 ± 1.6	3.5 ± 1.3 (n=45)	-	-	-
06 Mar	1.3 ± 0.5 (n=2)	2.4 ± 0.7	6.3 ± 2.1 (n=11)	2.8 ± 1.3 (n=5)	-	-
06 Dec	1.4 (n=1)	2.3 ± 0.7	6.6 ± 2.6 (n=129)	-	-	-
08 Jan	1.7 ± 0.4 (n=2)	1.8 ± 0.7	7.1 ± 2.1 (n=25)	4.3 ± 2.0 (n=5)	4.3 ± 1.1	3.2 ± 0.6 (n=8)

* Values corrected for the microtopographic relief of the sediment surface as suggested by Jørgensen and Des Marais (1990).

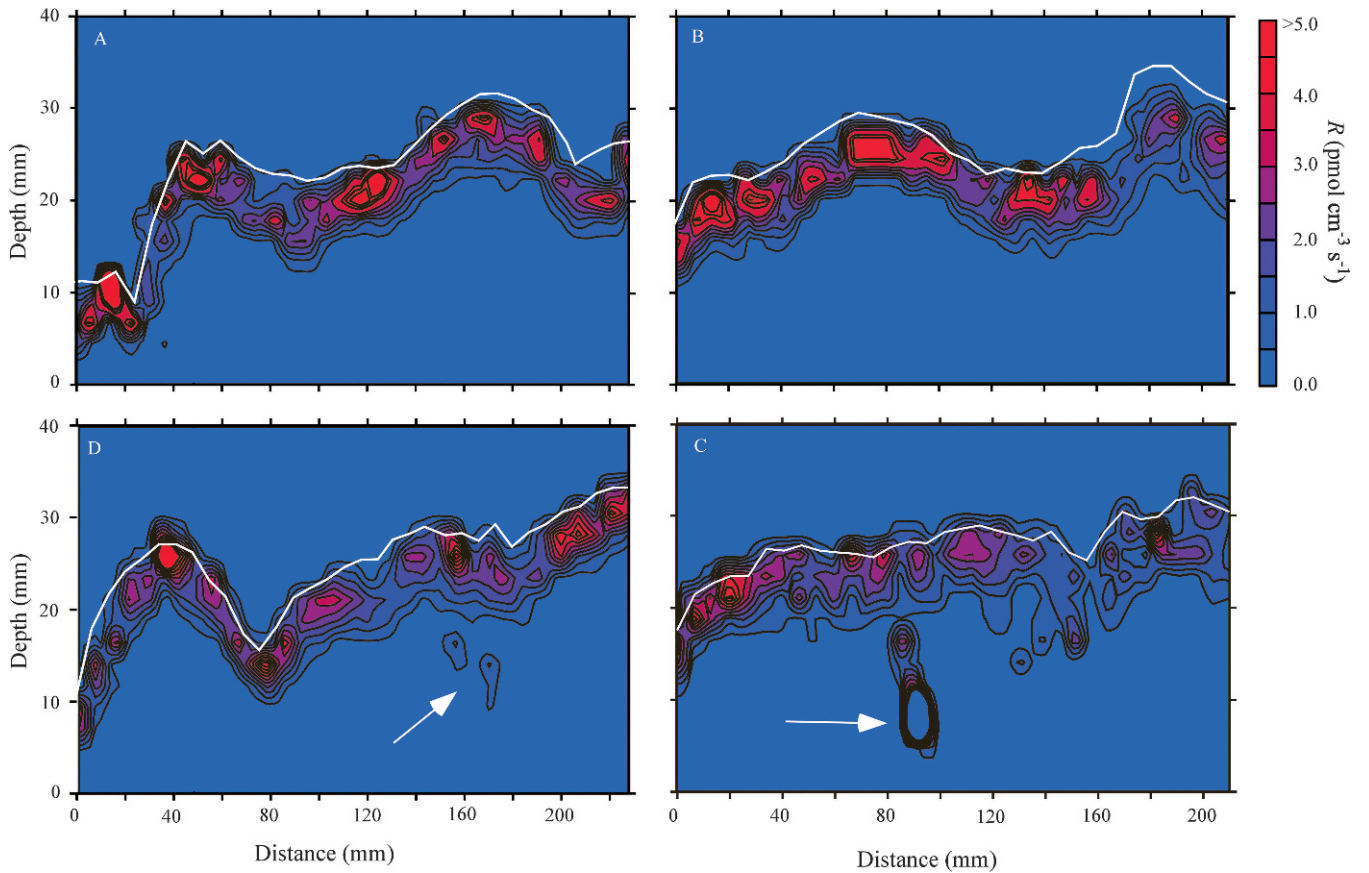


Fig. 7. (A–D) The calculated 2D volume-specific O₂ consumption rate, R , as calculated from the O₂ distribution of the four parallel transect presented in Fig. 6. The white line indicates the estimated position of the sediment surface and white arrows indicate penetrated infauna burrows.

marine-snow aggregates. The carbon deposition in central Sagami Bay is partly related to downslope transport of material (often of terrestrial origin) experiencing numerous resuspension cycles, and partly to a vertical transport of dense, fast-sinking marine snow aggregates from the photic

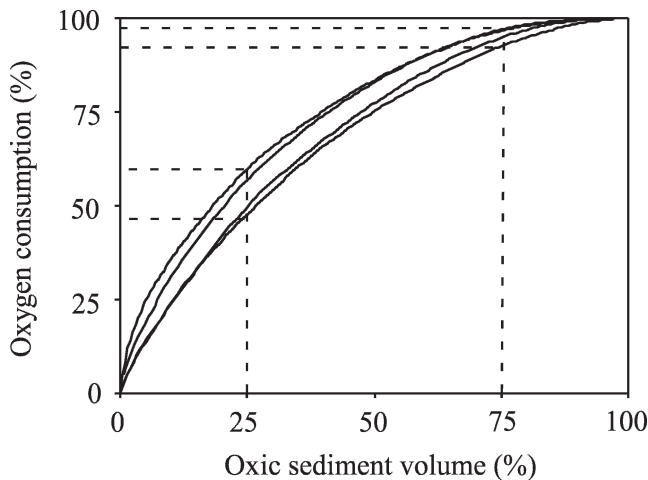


Fig. 8. The cumulative contribution of ranked sediment volumes to the total O₂ consumption for the four measured microtransects (see Fig. 7).

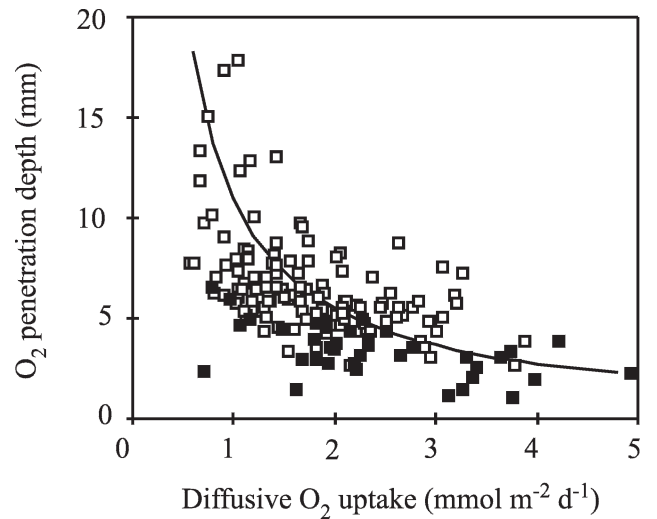


Fig. 9. The O₂ penetration depth, L , plotted as a function of the DOU as calculated from in situ O₂ microprofiles measured in September 2003 (black squares) and December 2006 (open squares). Measurements during late summer tend to be shifted toward the lower left corner. The solid line indicates the relation as predicted from $L = 2\phi D_s(C_w/DOU)$, (Cai and Sayles 1995); see text for details.

zone (Soh 2003). During our cruise, video recordings from the ROV revealed a very high particle density all through the water column and in the bottom water. Marine snow particles represent dynamic nutrient patches in the water column, typically with a turnover time on the order of days to weeks (Simon et al. 2002) and it has been shown that upon settlement marine snow parcels can induce short-lived benthic hot spots with intensified microbial activity (Glud 2008). The surface sediment of Sagami Bay is, thus, expected to host a suite of highly degradable to refractory organic carbon parcels. The hot spots identified in Fig. 7 probably represent a mixture of parcels with labile organic material originating from either marine snow or benthic infauna activity, potentially complemented by patches of upward-transported reduced sediment. This does imply that the micropatch structure is dynamic, with the respective electron donors of the parcel becoming exhausted and new parcels being formed. Recent work documented that short-term variability in the DBL structure can transplant down into the interstice and can cause dramatic changes in the benthic O_2 distribution (Glud et al. 2007), and this adds further to the complexity of characterizing conditions within such oxic surface sediments. Together this indicates that both temporal variations, on a scale of minutes–hours, and spatial variations, on a scale of millimeters–centimeters, can exceed a factor of 2–3, which is comparable to the seasonal variation published for many environments.

Even though the number of studies presenting in situ O_2 microprofiles is steadily increasing it is difficult to compare the present data set to any other data sets, because these generally only present a handful of microprofiles from a given location. Sometimes they express an intensive small-scale variability and some times not. At present we do not know to what extent the resolved micropatchiness is unique to central Sagami Bay or is representative for margin or marine sediments in general. The variability of aerobic activity may be relatively high in sediments with a low background activity and experiencing a dynamic and intense settlement of marine snow particles and/or rich in deposit-feeding infauna. However, the present study underpins that, in such sediments, multiple microsensor measurements are required to resolve the average condition, and that pore-water microprofiles of different solutes measured in parallel even in close vicinity to each other only should be vertically aligned with caution. Likewise, relating the occurrence of microorganisms or meiofauna to a single or even an averaged pore water–solute profile determined in parallel can be misleading. To the extent the present observations can be extrapolated beyond similar sediment types as studied here it conceptually affects our perspective on the function of surface sediments. The turnover of material may, to a large extent, be confined to highly active, local but diverse hot spots or zones with profound effect on the microbial ecology, procaryotic virus–host interactions and trophic coupling. Such an environment will presumably maintain a high microbial diversity, but also favors highly versatile organisms, motility, and efficient chemosensory behavior. Microbial dynamics and food-web structure of aerobic sediments may, thus, bear resemblance to conditions in the pelagic

environment where short-lived aggregates act as microbial hot spots with a relatively short turnover time (Blackburn et al. 1998; Seymour et al. 2005).

Benthic carbon mineralization in central Sagami Bay—

Even though early investigations suggested that the deep ocean margins represent areas of intensified benthic carbon mineralization (Jahnke et al. 1990; Walsh 1991) deep-slope sediments remain an understudied area of the ocean floor. The sediment of central Sagami Bay resides at a water depth of 1400–1500-m in a rounded deep basin surrounded by continental slopes, but connected to the deep Pacific Ocean via the Sagami Trough (Fig. 1). Even though the study area exhibit some special features it does bear resemblance to many marginal sediments along steep continental slopes and sediment of deep glacial fjords and, as such, it can be regarded as representative for such high-deposition areas.

We have determined the in situ DOU of central Sagami Bay on four occasions, while the TOU only was successfully measured during three of these visits. Parallel TOU and DOU measurements were in all cases not statistically different, indicating that the fauna irrigation only was of moderate importance for the benthic O_2 uptake (Table 1). However, laboratory-based measurements indicated elevated O_2 uptake rates (Table 1), presumably induced by artifacts related to sediment recovery as has been demonstrated in previous studies (Glud et al. 1994, 1999; Epping et al. 2002). The in situ microsensor measurements indicated a seasonal pattern with elevated benthic O_2 uptake (corrected for the microtopographic relief) of $3.3 \pm 1.6 \text{ mmol m}^{-2} \text{ d}^{-1}$ and a reduced O_2 penetration depth of $3.5 \pm 1.3 \text{ mm}$ during late summer as compared to the three winter campaigns with an average DOU of $2.2 \pm 0.7 \text{ mmol m}^{-2} \text{ d}^{-1}$ and an O_2 penetration of $6.7 \pm 2.5 \text{ mm}$ (Table 1). The bottom water O_2 concentration ranged in all instances between 55 and $59 \mu\text{mol L}^{-1}$ (data not shown). Extrapolating the summer and winter values to 6 months, respectively resulted in an average annual in situ DOU of $2.8 \text{ mmol m}^{-2} \text{ d}^{-1}$.

The average DOU of central Sagami Bay is at the high end of previous in situ ocean margin measurements performed at comparable depths (Archer and Devol 1992; Reimers et al. 1992; Sauter et al. 2001) and ranges with activities in the intense upwelling areas off Chile and Namibia (Glud et al. 1994, 1999). Based on a global compilation of available in situ O_2 microprofiles, DOU relates to the water depth (z) as $\text{DOU} = 84z^{-0.59}$ (Glud 2008), which would predict a DOU of $1.1 \text{ mmol m}^{-2} \text{ d}^{-1}$ for central Sagami Bay, which is only $\sim 50\%$ of the estimated average winter value derived from the microprofile DBL-gradient. The benthic activity of central Sagami Bay is relatively high and the data confirm the importance of deep margin sediments for regional carbon cycling (Jahnke et al. 1990; Walsh 1991).

The annual primary production for the area has been estimated to $33 \text{ mmol C m}^{-2} \text{ d}^{-1}$ and the average vertical organic carbon sedimentation as measured by sediment traps positioned 350 m above the seabed in the central bay amounts to $5.5 \text{ mmol C m}^{-2} \text{ d}^{-1}$ (Kanda et al. 2003). Assuming a respiratory quotient of 1.0 (i.e., one O_2 molecule consumed per CO_2 molecule produced), the

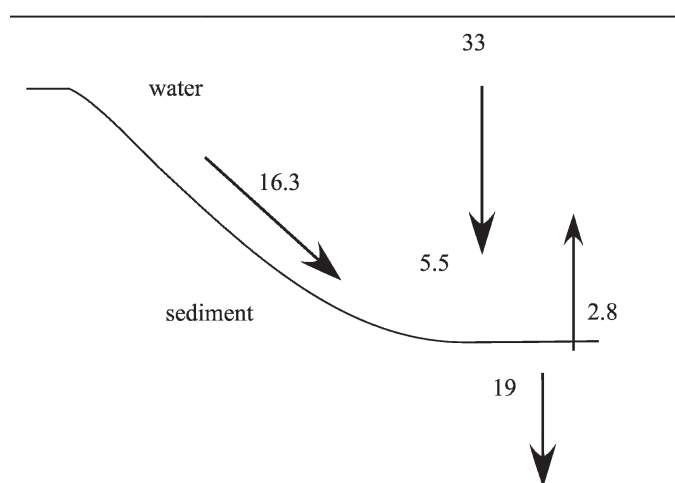
Carbon budget (mmol C m⁻² d⁻¹)

Fig. 10. An estimated carbon budget for central Sagami Bay. Please refer to the text for details on the calculations.

annual average DOU corresponds to the mineralization of ~50% of the organic carbon collected in the traps. However, the average annual organic carbon burial rates as calculated from the sediment organic carbon content measured at 10-cm sediment depth (*see above*) and the sediment accumulation rates derived from ²¹⁰Pb profiles (Kato et al. 2003) amounts to 19 mmol C m⁻² d⁻¹, which is retained in the sediment record. Even though this might be a relatively crude procedure because downslope transport of organic material may be very infrequent and erratic our estimates suggest that, on average, 16.3 mmol C m⁻² d⁻¹ (19 + 2.8 ± 5.5; Fig. 10) have other sources than that of vertically sinking organic matter. It also suggests that only ~10% of the organic carbon deposited in central Sagami Bay is mineralized within the upper 10 cm, while ~90% is retained in the deeper sediment layers or turned over at a very low rate below the active surface zone (Fig. 10). This is a relatively low mineralization efficiency, but aligns reasonable well with other environments of similar sediment accumulation rates (Canfield 1994) and most likely reflects the high input of refractory material. Even though deep margin sediments along steep continental slopes (as central Sagami Bay) represent areas with a relatively high carbon recycling rate they are also important regional zones for large-scale benthic carbon retention. They do, however, also represent dynamic environments that exhibit an extensive small-scale variability, which (at least the oxic zone) are best described as a mosaic of microbial zones and hot spots that are responsible for much of the diagenetic activity.

References

ALLER, R. C., P. O. J. HALL, P. D. RUDE, AND J. Y. ALLER. 1998. Biogeochemical heterogeneity and suboxic diagenesis in hemipelagic sediments of the Panama Basin. *Deep-Sea Res. Part I* **45**: 133–165.

- ARCHER, D., AND A. DEVOL. 1992. Benthic oxygen fluxes on the Washington shelf and slope: A comparison of in situ microelectrode and chamber flux measurements. *Limnol. Oceanogr.* **37**: 614–629.
- BERG, P., D. SWANEY, S. RYSGAARD, B. THAMDRUP, AND H. FOSSING. 2007. A fast numerical solution to the general mass-conservation equation for solutes and solids in aquatic sediments. *J. Mar. Res.* **65**: 317–343.
- BLACKBURN, B., T. FENCHEL, AND J. MITCHELL. 1998. Microscale nutrient patches in planktonic habitats shown by chemotactic bacteria. *Science* **282**: 2254–2256.
- BOUDREAU, B. P. 1997. Diagenetic models and their implementation. Springer-Verlag.
- CAI, W. J., AND F. L. SAYLES. 1995. Oxygen penetration depths and fluxes in marine sediments. *Mar. Chem.* **52**: 123–131.
- CANFIELD, D. E. 1994. Factors influencing organic carbon preservation in marine sediments. *Chem. Geol.* **114**: 315–329.
- COOK, P. L. M., F. WENZHÖFER, R. N. GLUD, AND M. HUETTEL. 2007. Benthic solute exchange and carbon mineralization in two shallow subtidal sandy sediments: Impact of advective porewater exchange. *Limnol. Oceanogr.* **52**: 1943–1963.
- EPPING, E. H. G., C. VAN DER ZEE, K. SOETAERT, AND W. HELDER. 2002. On the oxidation and burial of organic carbon in sediments of the Iberian and Nazare Canyon (NE Atlantic). *Mar. Ecol. Prog. Ser.* **52**: 399–431.
- FENCHEL, T. 1996. Worm burrows and oxic microniches in marine sediments. 2. Distribution patterns of ciliated protozoa. *Mar. Biol.* **127**: 297–301.
- . 2008. Motility of bacteria in sediments. *Aqua. Microb. Ecol.* **51**: 23–30.
- GLUD, R. N. 2008. Oxygen dynamics of marine sediments. *Mar. Biol. Res.* **4**: 243–289.
- , P. BERG, H. FOSSING, AND B. B. JØRGENSEN. 2007. Effect of the diffusive boundary layer (DBL) on the benthic mineralization and O₂ distribution: A theoretical modelling exercise. *Limnol. Oceanogr.* **52**: 547–557.
- , J. K. GUNDERSEN, AND O. HOLBY. 1999. Benthic *in situ* respiration in the upwelling area off central Chile. *Mar. Ecol. Prog. Ser.* **186**: 9–18.
- , ———, B. B. JØRGENSEN, N. P. REVSBECH, AND H. D. SCHULZ. 1994. Diffusive and total oxygen uptake of deep-sea sediments in the eastern South Atlantic Ocean: *In situ* and laboratory measurements. *Deep-Sea Res. Part I* **41**: 1767–1788.
- , J. K. GUNDERSEN, H. RØY, AND B. B. JØRGENSEN. 2003. Seasonal dynamics of benthic O₂ uptake in a semi-enclosed bay: Importance of diffusion and fauna activity. *Limnol. Oceanogr.* **48**: 1265–1276.
- , F. WENZHÖFER, A. TENGBERG, M. MIDDELBOE, K. OGURI, AND H. KITASATO. 2005. Distribution of oxygen in surface sediments from central Sagami Bay, Japan: *In situ* measurements by microelectrodes and planar optodes. *Deep-Sea Res. Part I* **52**: 1974–1987.
- GUNDERSEN, J. K., AND B. B. JØRGENSEN. 1990. Microstructure of diffusive boundary layers and the oxygen uptake of the seafloor. *Nature* **345**: 604–607.
- JAHNKE, R. A., C. E. REIMERS, AND D. B. CRAVEN. 1990. Intensification of recycling of organic matter at the seafloor near ocean margins. *Nature* **248**: 50–54.
- JØRGENSEN, B. B., AND D. J. DES MARAIS. 1990. The diffusive boundary layer of sediments: Oxygen microgradients over a microbial mat. *Limnol. Oceanogr.* **35**: 1343–1355.
- , R. N. GLUD, AND O. HOLBY. 2005. Oxygen distribution and bioirrigation in Arctic fjord sediments (Svalbard, Barents Sea). *Mar. Ecol. Prog. Ser.* **292**: 85–95.

- KANDA, J., S. FUJIWARA, H. KITAZATO, AND Y. OKADA. 2003. Seasonal and annual variation in the primary production regime in the central part of Sagami Bay. *Prog. Oceanogr.* **57**: 17–29.
- KATO, Y., H. KITAZATO, M. SHIMANAGA, T. NAKATSUKA, Y. SHIRAYAMA, AND T. MASUZAWA. 2003. ^{210}Pb and ^{137}Cs in sediments from Sagami Bay Japan: Sedimentation rates inventories. *Prog. Oceanogr.* **57**: 77–95.
- KITAZATO, H., AND OTHERS. 2003. Long-term monitoring of sedimentary processes in the central part of Sagami Bay, Japan: Rationale, logistics and overview of results. *Prog. Oceanogr.* **57**: 3–16.
- KUHL, M., AND N. P. REVSBECH. 2001. Biogeochemical micro-sensors for boundary layer studies, p. 180–210. *In* B. P. Boudreau and B. B. Jørgensen [eds.], *The benthic boundary layer*. Oxford Univ. Press.
- MIDDELBOE, M., R. N. GLUD, F. WENZHÖFER, K. OGURI, AND H. KITAZATO. 2006. Spatial distribution and activity of viruses in deep-sea sediments of Sagami Bay, Japan. *Deep-Sea Res. Part I* **53**: 1–13.
- PRECHT, E., U. FRANKE, L. POLERECKY, AND M. HUETTEL. 2004. Oxygen dynamics in permeable sediments with a wave-driven pore water exchange. *Limnol. Oceanogr.* **49**: 693–705.
- RABOUILLE, C., L. DENIS, K. DEDIEU, G. STORA, B. LANSARD, AND C. GRENZ. 2003. Oxygen demand in coastal marine sediments: Comparing in situ microelectrodes and laboratory core incubations. *J. Exp. Mar. Biol. Ecol.* **285–286**: 49–69.
- RASMUSSEN, H., AND B. B. JØRGENSEN. 1992. Microelectrode studies of seasonal oxygen uptake in a coastal sediment: Role of molecular diffusion. *Mar. Ecol. Prog. Ser.* **261**: 289–303.
- REIMERS, C. E., R. A. JAHNKE, AND D. E. MCCORKLE. 1992. Carbon fluxes and burial rates over the continental slope and rise off central California with implications for the global carbon cycle. *Glob. Biogeochem. Cyc.* **6**: 199–224.
- REVSBECH, N. P. 1989. An oxygen microelectrode with a guard cathode. *Limnol. Oceanogr.* **34**: 474–478.
- RØY, H., M. HÜTTEL, AND B. B. JØRGENSEN. 2005. The influence of topography on the functional exchange surface of marine soft sediments, assessed from sediment topography measured in situ. *Limnol. Oceanogr.* **50**: 106–112.
- SAUTER, E. J., M. SCHLÜTER, AND E. SUESS. 2001. Organic carbon flux and remineralization in surface sediments from the northern North Atlantic derived from pore-water oxygen microprofiles. *Deep-Sea Res. Part I* **48**: 529–553.
- SEYMOUR, J. R., L. SEURONT, AND J. G. MITCHELL. 2005. Microscale and small-scale temporal dynamics of a coastal planktonic microbial community. *Mar. Ecol. Prog. Ser.* **300**: 21–37.
- SIMON, M., H. P. GROSSART, B. SCHWEITZER, AND H. PLOUG. 2002. Microbial ecology of organic aggregates in aquatic ecosystems. *Aquat. Microb. Ecol.* **28**: 175–211.
- SOH, W. 2003. Transport processes deduced from geochemistry and the void ratio of surface core samples, deep sea Sagami Bay, central Japan. *Prog. Oceanogr.* **57**: 109–124.
- THAMDRUP, B. 2000. Bacterial manganese and iron reduction in marine sediments. *Adv. Microb. Ecol.* **16**: 41–94.
- ULLMAN, W. J., AND R. C. ALLER. 1982. Diffusion coefficients in near-shore marine sediments. *Limnol. Oceanogr.* **27**: 552–556.
- WALSH, J. J. 1991. Importance of continental margins in the marine biogeochemical cycling of carbon and nitrogen. *Nature* **350**: 53–55.
- WENZHÖFER, F., AND R. N. GLUD. 2004. Small-scale spatial and temporal variability in benthic O_2 dynamics of coastal sediments: Impact of fauna activity. *Limnol. Oceanogr.* **49**: 1471–1481.
- ZHU, Q. Z., R. C. ALLER, AND Y. Z. FAN. 2006. Two dimensional pH distributions and dynamics in bioturbated marine sediments. *Geochim. Cosmochim.* **70**: 4933–4949.

Edited by: Jack J. Middelburg

Received: 03 June 2008

Accepted: 19 August 2008

Amended: 28 August 2008